DOI 10.1007/s10891-017-1578-x
Journal of Engineering Physics and Thermophysics, Vol. 90, No. 2, March, 2017

TRANSFER PROCESSES IN LOW-TEMPERATURE PLASMA

NUMERICAL STUDY OF PARTICLE HEATING IN A PLASMA JET

A. Essiptchouk,[a] G. Petraconi,[b] F. R. Caliari,[c] F. S. Miranda,[b] M. Yesipchuk,[d] and A. Petraconi[e]

UDC 536.2

The motion of particles axially injected into the plasma spray process has been studied using a one-dimensional model. The effect of the initial particle velocity and particle diameter on the final particle velocity and temperature was evaluated. The aim of the work is to optimize the spraying process by defining the favorable particle injection velocity, considering a wide range of velocity and temperature of the plasma jet.

Keywords: *high-velocity plasma spray, cold spray, plasma powder spraying, computer modeling, process control.*

Introduction. The velocity and temperature of particles in the plasma spray process depend strongly on their interaction with a high-temperature plasma jet. The in-flight particle properties, before collisions with a substrate, influence the coating quality. In a conventional atmospheric plasma spray process [1, 2], good adhesion of coating is obtained when a particle is heated up to the temperature window (interval) between the melting and evaporation points. On the other hand, the particle velocity must be high enough to provide good adherence, but not too large in order not to cause fragmentation of a sprayed particle.

It is not always necessary to attain the melting state of a particle. The recently described cold spray coating process [3] belongs to the family of the thermal spray processes [2], and it is characterized by a reduced particle temperature and elevated velocities. In this case, instead of the thermal particle energy, the kinetic energy gained allows one to form good adhesion with a substrate by plastic particle deformation during the collision. The main advantage of a cold spray is the minimization of the undesirable temperature effects, like melting, evaporation, oxidation, crystallization, residual stresses, gas release, etc. [4].

Recently, a new design of a plasma torch (High Velocity Plasma Spray or HVPS) was presented [5] which allows one to combine the advantages of kinetic and thermal processes. This plasma torch is characterized by axial injection of particles into a subsonic flow with subsequent acceleration in a plasma jet up to supersonic velocities. Moreover, the improved arc stability (the arc length is physically fixed, which provides low arc fluctuations) and the increased plasma jet enthalpy (due to the high pressure in the plasma torch discharge chamber) allow one to expand the variety of powder materials (metals and ceramics) used in the process, as well as to improve the quality of a coated surface (an increase in the particle velocity reduces the porosity of the coated layer).

In many cases, the process parameters (like the plasma jet temperature, particle velocity and temperature, melting index, etc.) are tightly interconnected, and the effects of this interaction are quite complex. In this work, a simplified one-dimensional model is used to investigate the effect of the initial particle velocity on the particle heating and acceleration processes with consideration of different plasma jet characteristics. The intention of the work is to determine the process window (i.e., the final particle temperature and velocity) in order to optimize the HVPS process.

Computational Model and Preliminary Assumptions. *Assumptions.* The simulation was carried out by using a one-dimensional model with consideration of particles injected axially into a plasma jet with a constant velocity. Two jet

[a]Instituto de Ciência e Tecnologia, UNESP — Universidade Estadual Paulista, 12247-004 São José dos Campos, SP, Brazil; email: alexei.essiptchouk@gmail.com; [b]Plasma and Processes Laboratory, Department of Physics, Technological Institute of Aeronautics, 12228-900, ITA–DCTA, São José dos Campos, SP, Brazil; [c]Universidade Federal de São Paulo, São José dos Campos, SP, Brazil; [d]Laboratory of Forest and Petrochemical Products, Institute of Chemistry of New Materials, National Academy of Sciences of Belarus, Minsk, Belarus; [e]Mogi das Cruzes University, Mogi das Cruzes, SP 08780-911, Brazil. Published in Inzhenerno-Fizicheskii Zhurnal, Vol. 90, No. 2, pp. 423–430, 2017. Original article submitted April 11, 2016.

velocities, u_g = 400 and 1000 m/s, were examined, and the particle injection velocity range v_{p0} = 0–1200 m/s was taken into account. A trace amount of particles was injected; thus the plasma properties, such as, for example, the plasma temperature T_{pl} = 3000 K, remained constant. Air was assumed to be a plasma-forming gas, and its thermodynamic properties were taken from [6]. Spherical particles with the diameter range d_p = 10–60 μm were selected as a model material. The particle properties, i.e., the specific mass ρ = 5890 kg/m^3 and the specific heat c_p = 466 J/(kg·K) were taken from the data for yttria-stabilized zirconia (YSZ).

Model. The theoretical background of particle motion and heating in a high-velocity and high-enthalpy plasma jet have been described in, for example, [1, 2, 7]. The particle motion is determined by the balance of the forces acting on the particle with mass m_p and defined as

$$\mathbf{F}_i = \sum \mathbf{F}_j \ . \tag{1}$$

The inertia force $\mathbf{F}_i = m_p \dfrac{dv_p}{dt}$ is equilibrated by the vector sum of all the external forces $\mathbf{F}_j$, such as the viscous drag force, plasma pressure gradient force, drag force due to the "added mass" (Archimedean one), Basset history term (due to the nonsteady particle motion), external potential forces (gravity, electric or magnetic forces), as well as the turbulence and thermophoretic forces. In most cases under study, the viscous drag force $\mathbf{F}_{d.f}$ originating from the shear stress occurring in a fluid near an immersed object exerts the major influence. It is given by

$$\mathbf{F}_{d.f} = C_D \frac{\rho_g \mathbf{U}^2}{2} A_p \ . \tag{2}$$

Here, C_D is the drag coeficient, A_p is the frontal area of the particle, ρ_g is the plasma gas density, and $\mathbf{U} = \mathbf{u}_g - \mathbf{v}_p$ is the particle velocity relative to the plasma jet velocity. In order to take into account the particle acceleration or deceleration, the square of the velocity **U** is written as follows:

$$\mathbf{U}^2 = \left(\mathbf{u}_g - \mathbf{v}_p\right)\left|\mathbf{u}_g - \mathbf{v}_p\right| . \tag{3}$$

The drag coefficient C_D is a function of the relative particle velocity **U** and is usually determined in terms of the particle Reynolds number Re defined by

$$\mathrm{Re} = \frac{\rho_g d_p \left|u_g - v_p\right|}{\mu_g} , \tag{4}$$

where μ_g is the dynamic plasma viscosity.

For different ranges of Re, one can find diverse approximations of $C_D = f(\mathrm{Re})$ (see, for example, [2, 7]). In this simulation, the so-called White approximation of the drag coefficient [8], proposed for the flows with low Reynolds numbers, is used:

$$C_D(\mathrm{Re}) = \frac{24}{\mathrm{Re}} + \frac{6}{1+\sqrt{\mathrm{Re}}} + 0.4 \ . \tag{5}$$

Thus, the differential equation of the particle motion in a high-temperature plasma jet is given as

$$\frac{dv_p}{dt} = \frac{\rho_g}{d_p \rho_p}\left(\frac{18}{\mathrm{Re}} + \frac{4.5}{1+\sqrt{\mathrm{Re}}} + 0.3\right)\left(u_g - v_p\right)\left|u_g - v_p\right| . \tag{6}$$

The Biot number was assumed to be small enough in a heat transfer phenomenon occurring between a particle and plasma jet. Accordingly, the one-temperature model of the particle, where any temperature gradient inside it is absent, is used. Moreover, the heat loss due to radiation and phase transformation was neglected, so the particle temperature was determined from the equation

$$m_p c_p \frac{dT_p}{dt} = A_p h_p \left(T_g - T_p\right) . \tag{7}$$

The particle mass $m_p = \dfrac{1}{6}\pi d_p^3 \rho$, its frontal area $A_p = \pi d_p^2$, and the specific heat c_p were assumed to be constant, i.e., independent of the temperature and processing time. The heat transfer coefficient h_p becomes available from the Nusselt number. For a spherical particle [7]

$$\mathrm{Nu} = \frac{h_\mathrm{p} d_\mathrm{p}}{\lambda_\mathrm{t}} = 2 + 0.66\mathrm{Re}^{0.5}\mathrm{Pr}^{0.33} \ . \tag{8}$$

Here, the Prandtl number $\mathrm{Pr} = \dfrac{\mu_\mathrm{g} c_{p\mathrm{g}}}{\lambda_\mathrm{g}}$ is calculated from the plasma gas properties at temperature T_pl; μ_g, λ_g, and $c_{p\mathrm{g}}$ are the dynamical viscosity, thermal conductivity, and the specific heat of a plasma gas, respectively. The average thermal conductivity of the particle is calculated as

$$\lambda_\mathrm{t} = \frac{1}{T_\mathrm{g} - T_\mathrm{p}} \int_{T_\mathrm{p}}^{T_\mathrm{g}} \lambda_\mathrm{t}(T) dT \ . \tag{9}$$

With the above-mentioned assumptions, the final differential equation for the temporal variation of the particle temperature is given by

$$\frac{dT_\mathrm{p}}{dt} = \frac{6\lambda_\mathrm{t}}{\rho_\mathrm{p} c_\mathrm{p} d_\mathrm{p}^2} \left(2 + 0.66\mathrm{Re}^{0.5}\mathrm{Pr}^{0.33}\right)\left(T_\mathrm{g} - T_\mathrm{p}\right). \tag{10}$$

Equations (6) and (10) form a closed system that permits one to obtain (using standard commercial software) the velocity and temperature of a particle at any instant of flight.

Results and Discussion. The system of differential equations (6) and (10) was solved by considering the range of the particle diameters d_p from 10 to 60 μm with a step of 10 μm at the fixed plasma jet temperature T_pl = 3000 K and with taking into account two plasma jet velocities u_g (400 and 1000 m/s). Such velocities were chosen in order to identify a possible deviation in the behavior of a particle during its heating and acceleration. The last velocity value of the plasma jet is nearly equal to the sonic velocity at T_pl. Obviously, in the vicinity of the sound velocity, the drag force and heat transfer coefficient will deviate from the empirical formulas used in this work. Nevertheless, the model permits revealing the general behavior of the particle parameters.

Figure 1a shows the particle velocity variation along the distance for the particle diameters 20 and 60 μm and different initial velocities. The highest velocity variation (increment or decrease) $\Delta v = \left|v_\mathrm{p.fin} - v_\mathrm{p0}\right|$ is achieved with the particle injection velocity v_p0 = 0. At a flight distance of 0.2 m, the final particle velocity $v_\mathrm{p.fin}$ increased up to 150 m/s, which corresponds to 38% of the plasma velocity.

With increase in the particle injection velocity, Δv diminishes until it attains the zero value for a trivial case of $v_\mathrm{p0} = u_\mathrm{g}$, when the drag force is zero. For v_p0 greater than the plasma jet velocity, the final velocity is not affected so much. For example, for v_p0 = 750 m/s the decrease in the initial particle velocity with a diameter of 60 μm is relatively small and attains the value Δv = 20 m/s, or 5% of the plasma velocity.

With decrease in the particle diameter, the velocity variation Δv increases. For a particle with a diameter of 20 μm and v_p0 = 0, the velocity increases up to v_p = 285 m/s (which corresponds to 71% of the plasma velocity), as can be observed in Fig. 1a. However, when the particle injection velocity is v_p0 = 750 m/s, the final particle velocity decreases by about 15%.

The behavior of the particle temperature vs. the distance from the injection nozzle is shown in Fig. 1b. The plasma jet temperature is assumed to be 3000 K. For a low particle injection velocity, one can observe an asymptotic increase in the particle temperature. Small particles can be heated to the temperature close to the plasma one at relatively small flight distances. With increase in v_{p0}, the flight time and heat transfer coefficient diminish and the particle requires a larger flight distance to attain the desired temperature. With increasing particle diameter (mass), the situation is impaired.

From the differential equations (6) and (7), one can conclude that both the particle acceleration and temperature are connected with the relative velocity Δv of the plasma jet and particle. The particle velocity is directly proportional to Δv, i.e., $\dfrac{dv_\mathrm{p}}{dt} \sim \dfrac{\Delta v}{d_\mathrm{p}^2}$, whereas the particle temperature is less influenced, namely, $\dfrac{dT_\mathrm{p}}{dt} \sim \dfrac{|\Delta v|^{0.5}}{d_\mathrm{p}^{1.5}}$. The particle acceleration or deceleration depends on the sign of Δv and increases with Δv. The rate of the particle temperature change is always positive due to the fact that the Reynolds number involves an absolute value of the velocity. Therefore the particles with zero injection velocity have higher acceleration than those with nonzero one. However, in the case of $v_\mathrm{p0} > u_\mathrm{g}$ the inertial force of the particle is sufficiently high, while the time of its interaction with a plasma jet is short, which results in a weak reduction in the initial particle velocity.

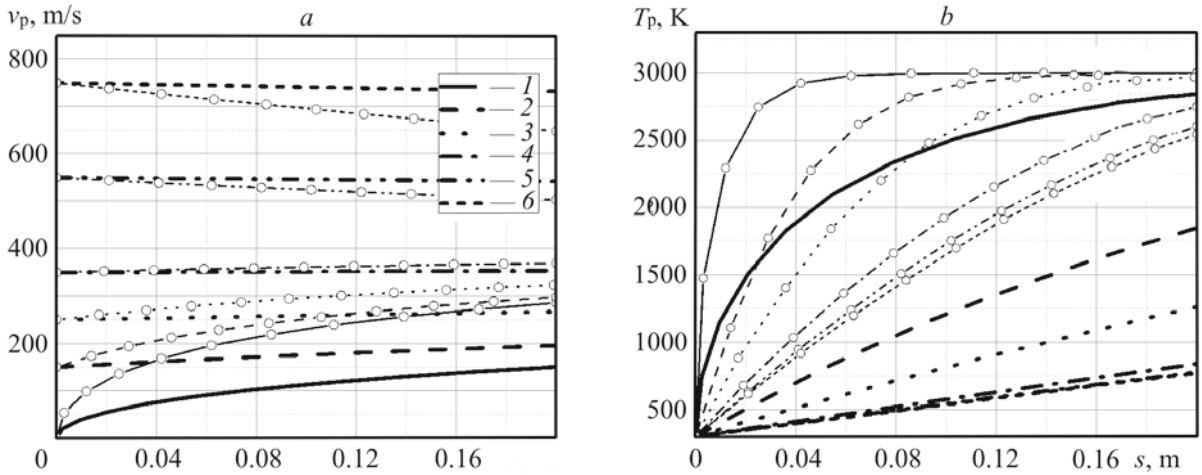

Fig. 1. Particle velocity (a) and temperature (b) at the plasma jet velocity 400 m/s vs. the flight distance for the particle diameter 60 μm (curves without symbols) and 20 μm (curves with symbols) and different particle injection velocities: 1) 0; 2) 150; 3) 250; 4) 350; 5) 550; 6) 750 m/s.

Competition between the rate of the velocity change and the particle heating rate results in a rapid decrease in the final particle temperature at a fixed flight distance. The particle acceleration and heating rate are inversely proportional to the particle diameter in powers 2 and 1.5, respectively. Thus, under the conditions studied, the particle diameter has a greater influence on the particle velocity than on the temperature.

The particle velocity and temperature variations as functions of the initial particle velocity and particle diameter are shown in Fig. 2 for two plasma velocities, 400 and 1000 m/s. In all cases, an increase in v_{p0} results in an increase in the final particle velocity which asymptotically approaches a linear function, practically independent of the plasma jet velocity, as follows from the model used (see Eq. (6)). Splitting of the final particle velocity with diameter occurs for low injection velocities. The highest separation is observed in the case of $v_{p0} = 0$. With increase in v_{p0}, the velocity dispersion decreases until all the particles with different diameters attain the same velocity. This occurs when $v_{p0} = u_g$ and the drag force vanishes. In the case of $v_{p0} > u_g$, a new particle splitting is observed, but it is relatively weak. This result shows the advantage of using high velocities, which allows one to obtain a flow of particles with different diameters and a more uniform distribution of velocities $v_{p.fin} = f(d_p)$.

Figure 2b shows the temperature variation of the particle after it covers the distance 0.1 m in a plasma jet as a function of the initial velocity. The results of calculating for particles of different diameters are shown. A strong decrease in the particle temperature for $v_{p0} < u_g$ is clearly observed in this figure. A local minimum of the particle temperature is reached for $v_{p0} = u_g$, when heat transfer occurs only by conduction (which is indirectly taken into account in this model), whose intensity is much lower compared to forced convection. After the particle arrives at this point, its temperature has little influence on the particle injection velocity.

It is interesting to observe that, after a certain value of v_{p0}, the temperature of the decelerated particle (for $v_{p0} > u_g$ in a plasma flow with $u_g = 400$ m/s) surpasses the temperature of the accelerated particle (a plasma flow with $u_g = 1000$ m/s). This result shows that the particle heating process, at elevated injection velocities and determined flight distance, is more effective in plasma flows with lower velocities. In the case studied, the critical value of the injection velocity takes place in the range between 650 and 700 m/s. This critical injection velocity grows slightly with the particle diameter.

The influence of the particle diameter on the particle temperature and velocity is shown in Fig. 3. The initial particle velocity was assumed to be $v_{p0} = 0$. This figure shows that an increase in the particle diameter diminishes both the particle velocity (due to the growing mechanical inertia) and the temperature (due to the increase in the thermal storage capacity). Moreover, for the case of a higher-velocity plasma jet, all the particles are well accelerated, whereas their temperature is smaller compared with that for a lower-velocity jet. The final particle velocity $v_{p.fin}$ achieved at a flight distance of 0.1 m decreases by 50% when the diameter changes from 20 to 60 μm, and this result is practically independent of the plasma jet velocity. However, the final particle temperature is strongly dependent on the jet velocity. The increase from 400 to 1000 m/s

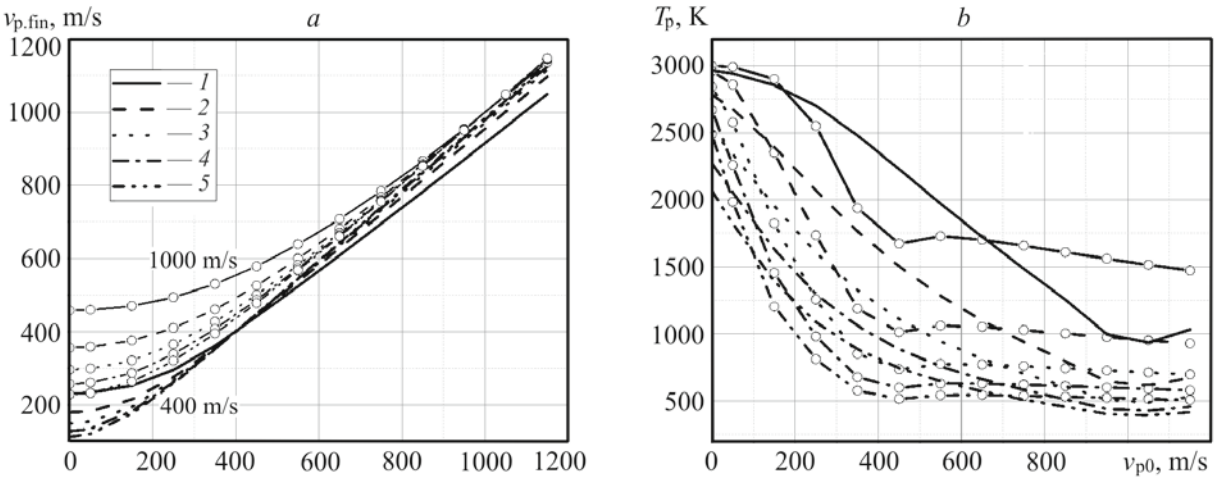

Fig. 2. Particle velocity (a) and temperature (b) at a distance of 0.1 m from the injection point versus the particle injection velocity for the plasma jet velocity 400 m/s (curves without symbols) and 1000 m/s (curves with symbols) and different particle diameters: 1) 20; 2) 30; 3) 40; 4) 50; 5) 60 μm.

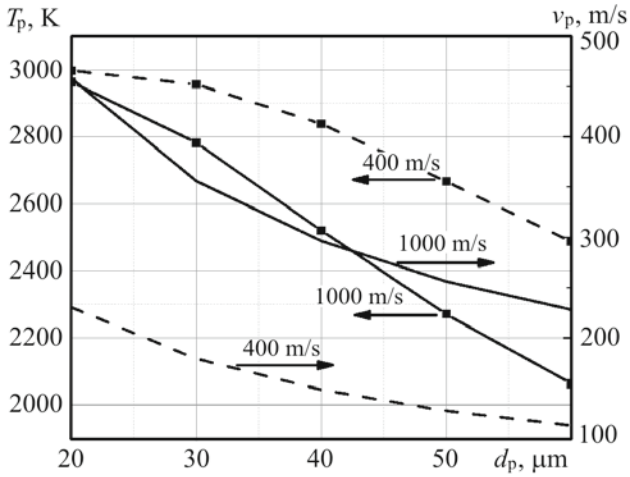

Fig. 3. Particle velocity and temperature at a distance of 0.1 m from the injection point as functions of the particle diameter at zero particle injection velocity for different plasma jet velocities.

results in the rise of the temperature difference between particles of diameters d_1 and d_2, i.e., $\Delta T = T(d_1 - T(d_2)$. For the particle diameters d_1 = 20 μm and d_2 = 60 μm, the temperature difference varies from 17% (for u_g = 400 m/s) to 30% (for u_g = 1000 m/s).

For comparison, instead of using the absolute values of the particle velocity v_p and temperature T_p, both the heating and acceleration processes can be analyzed in terms of the kinetic energy $E_K = \frac{m_p v_p^2}{2}$ and the thermal energy $E_T = m_p c_p (T_p - T_{p0})$. Moreover, in order to generalize the results, the specific values of the energy per unit mass will be applied, i.e., the specific kinetic energy $e_K = \frac{v_p^2}{2}$ and the specific thermal energy $e_T = c_p(T_p - T_{p0})$, both in J/kg. Figure 4 shows the impact of the particle injection velocity on the specific energy (kinetic, thermal, and total, where $e_{tot} = e_K + e_T$). Two particle diameters were chosen as representative, namely, d_p = 20 and 60 μm, and the energies were evaluated in the plasma jets with the velocities 400 m/s (Fig. 4a) and 1000 m/s (Fig. 4b). Figure 4 shows that the kinetic energy increases with the particle injection velocity, whereas the thermal energy decreases. Under this condition, a minimum in the total energy occurs.

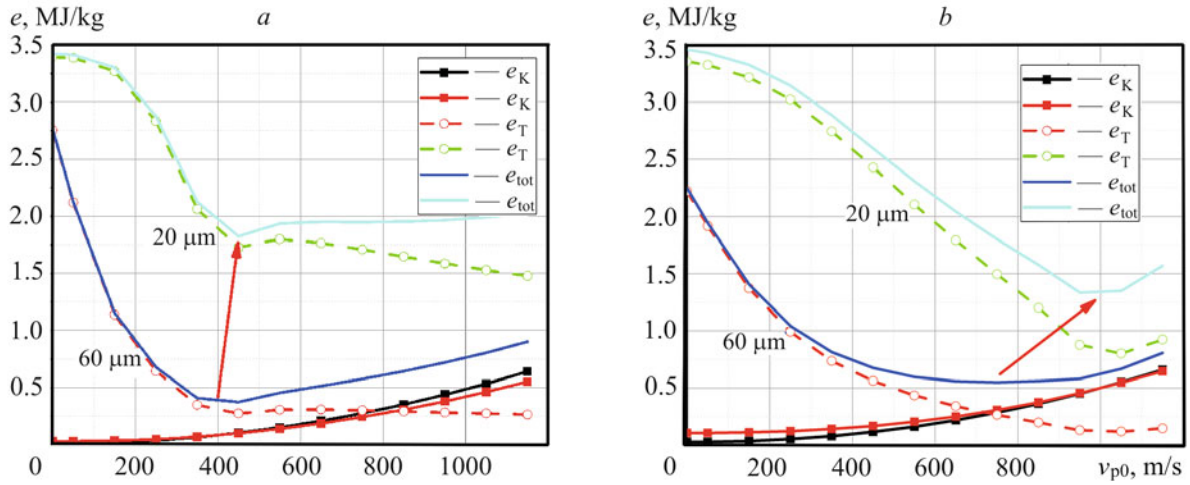

Fig. 4. Specific particle energies as functions of the particle injection velocity at a distance of 0.1 m from the injection point for different particle diameters at u_g = 400 m/s (a) and 1000 m/s (b).

Considering the case of the plasma velocity u_g = 400 m/s, we see that a minimum total energy occurs in the vicinity of u_g and it varies slightly with the particle diameter. The specific thermal energy forms the principal part of the total one. The specific kinetic energies for two values of the particle diameter are almost identical (cf. Fig. 2a). The same dependence is observed in the case of the high velocity plasma jet. Figure 4 shows that a minimum of the total energy shifts to lower values of v_p with increase in the particle diameter.

To estimate the effect of both the plasma velocity and particle diameter on the total specific energy, two parameters are introduced. The first of them,

$$\alpha_{d_{p1}/d_{p2}} = \frac{e_{tot}\big|_{d_{p1}}}{e_{tot}\big|_{d_{p2}}},$$

represents the total specific energy gained by the particle of diameter d_{p1} against the energy gained by the particle with diameter d_{p2} in a plasma flow with a constant velocity u_g. Another parameter,

$$\beta_{u_{g1}/u_{g2}} = \frac{e_{tot}\big|_{u_{g1}}}{e_{tot}\big|_{u_{g2}}},$$

shows the total specific energy of the particle of diameter d gained in a plasma flow with a velocity u_{g1} against the total energy gained by the same particle in a plasma flow with a velocity u_{g2}.

Figure 5 shows the influence of the initial particle velocity on the parameters α and β. In the calculations, the particle diameters d_{p1} = 20 μm and d_{p2} = 60 μm and the plasma velocities u_{g1} = 400 m/s and u_{g2} = 1000 m/s were used. The flight distance was 0.1 m. From Fig. 5a it can be noticed that the energy of the particle with the diameter 20 μm practically always exceeds that for the diameter 60 μm (α > 1) with the maximum value of α equal to 5 for u_g = 400 m/s and nearly 4 for u_g = 1000 m/s. Both maxima are located between 350 and 550 m/s. An increase in u_g diminishes the parameter α and shifts its maximum value to the highest values of v_{p0}.

Figure 5b gives the effect of v_{p0} on the parameter β. It is evident that for the injection velocity range 100–700 m/s the plasma jet with u_g = 1000 m/s makes a much greater contribution to the total energy of particles (β < 1). Outside of this range, the plasma flow with a lower velocity is still more effective for the increase in the total energy of particles. This result is explained by the higher absolute difference between the plasma and particle velocities, i.e., $|u_g - v_p|$, which contributes to the thermal energy.

The change of the total specific particle energy with the particle injection velocity is shown in Fig. 6, where the normalized quantities are used. The enthalpy of the plasma jet, h = 3.79 MJ/kg for T = 3000 K [6], was adopted as a basis for

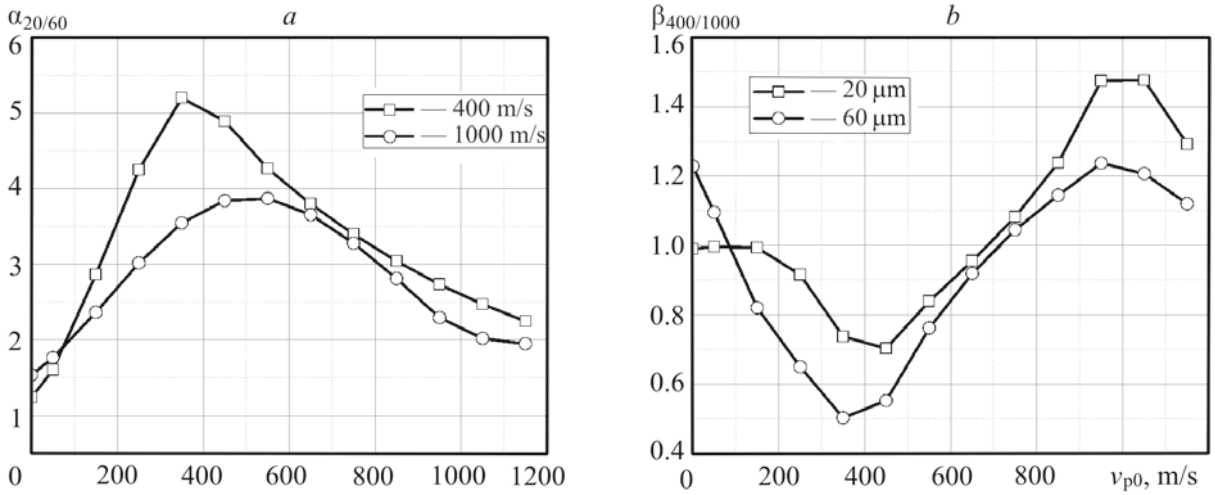

Fig. 5. Dimensionless parameters α (a) and β (b) vs. the particle injection velocity for different plasma jet velocities (a) and different diameters (b).

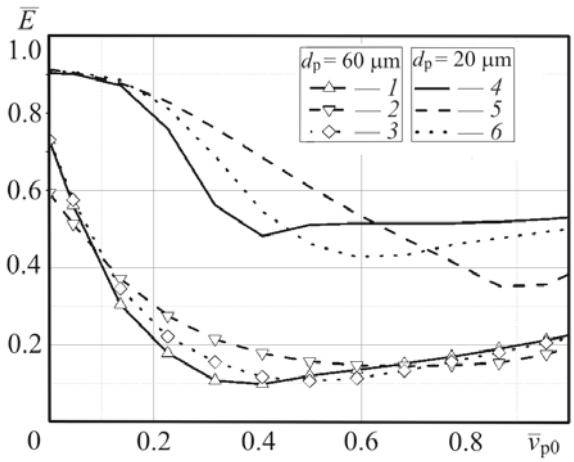

Fig. 6. Normalized particle energy vs. the particle injection velocity at a flight distance of 0.1 m for different plasma jet velocities: 1, 4) 400 m/s; 2, 5) 1000 m/s; 3, 6) linear velocity increment from 400 to 1098 m/s.

the calculation of the normalized energy $\bar{E} = e_{\text{tot}}/h$. The sound velocity in air at the plasma temperature (a_{ar} = 1098 m/s) was used as a basis for the normalized velocity calculations, i.e., $\bar{v}_{\text{p0}} = v_{\text{p0}}/v_{\text{ar}}$.

Two particles diameters, 20 and 60 μm, form two distinguishable sets of data, as shown in Fig. 6. Each set of data presents the normalized particle energy modeled for the constant plasma jet velocities 400 and 1000 m/s, as well as for the plasma velocity linearly increased from 400 m/s (at the injection point) to the sound velocity at the flight distance 0.1 m. From Fig. 6 it can be observed that the highest value of the total particle energy is achieved only if the initial particle velocity is equal to zero. The particle diameter has the major influence on the energy in comparison with the particle injection velocity. The application of supersonic jets will change the scenario presented in this work due to the variation in the drag coefficient and heat transfer.

Conclusions. Within the framework of the model considered, it can be concluded that an increase in the initial particle velocity for a plasma jet with constant velocity and temperature significantly reduces the particle temperature which, in turn, determines the total particle energy. When the particle injection velocity is higher than the plasma jet velocity, the kinetic energy contribution begins to equalize with the thermal particle energy (for particles of low diameters) or even to

exceed it (in the case of particles with larger diameters). For the model used, the particle reaches the highest total energy (kinetic and thermal) only when the injection velocity is equal to zero.

NOTATION

A_p, frontal particle area, m^2; a_{ar}, sound velocity of air, m/s; C_D, drag coefficient; c_p, specific heat of the particle material, J/(kg·K); c_{pg}, specific heat of plasma, J/(kg·K); d_p, d_1, d_2, particle diameters, μm; E_K, kinetic energy, J; E_T, thermal energy, J; e_K, specific kinetic energy, J/kg; e_T, specific thermal energy, J/kg; e_{tot}, total specific energy, J/kg; $\mathbf{F}_i$, $\mathbf{F}_j$, $\mathbf{F}_{d.f}$, inertia forces, external forces, and viscous drag force, respectively, N; h, enthalpy of plasma, J/kg; h_p, convection heat transfer coefficient, W/(m^2·K); m_p, particle mass, kg; Nu, Nusselt number; Pr, Prandtl number; T_{pl}, plasma temperature, K; Re, Reynolds number; **U**, particle velocity relatively to the plasma jet velocity, m/s; $\mathbf{u}_g$, plasma jet velocity, m/s; $\mathbf{v}_p$, particle velocity, m/s; $\mathbf{v}_{p0}$, initial particle velocity, m/s; $\mathbf{v}_{p.fin}$, final particle velocity, m/s; Δv, velocity variation, m/s; $\alpha_{d_{p1}/d_{p2}}$, $\beta_{u_{g1}/u_{g2}}$, dimensionless parameters for the total specific energy gain in a plasma flow with a constant plasma velocity and particle diameter, respectively; λ_g, thermal conductivity of plasma, W/(m·K); λ_t, average thermal conductivity of a particle, W/(m·K); μ_g, dynamic viscosity of plasma, N·s/m^2; ρ, specific mass (density) of a particle, kg/m^3; ρ_g, plasma gas density, kg/m^3. Indices: g, plasma gas; i, inertia; p, particle; pl, plasma; tot, total.

REFERENCES

1. R. B. Heimann, *Plasma-Spray Coating: Principles and Applications*, Wiley-VCH, Weinheim (1996).
2. P. Fauchais, J. Heberlein, and M. I. Boulos, *Thermal Spray Fundamentals from Powder to Part*, Springer, New York (2013).
3. A. Papyrin, V. Kosarev, S. Klinkov, A. Alkhimov, and V. Fomin, *Cold Spray Technology*, Elsevier, Amsterdam (2006).
4. H. Singh, T. S. Sidhu, and S. B. S. Kalsi, Cold spray technology: future of coating deposition processes, *Fract. Integr. Struct.*, **22**, 69–84 (2012).
5. F. R. Caliari, F. S. Miranda, D. A. P Reis, G. P. Filho, L. I. Charakhovski, and A. M. Essiptchouk, New kind of plasma torch for supersonic coatings at atmospheric pressure, in: *Proc. 22nd Int. Symp. on Plasma Chemistry*, 5–10 July, 2015, Antwerp, Belgium: http://www.ispc-conference.org/index.php/proceedings/
6. M. I. Boulos, P. Fauchais, and E. Pfender, *Thermal Plasmas. Fundamentals and Applications*, Springer (1994).
7. L. Pawlowski, *The Science and Engineering of Thermal Spray Coatings*, John Wiley & Sons Ltd. (2008).
8. F. M. White, *Viscous Fluid Flow*, McGraw Hill Inc., New York (1974).